Journal of the Electrochemical Society

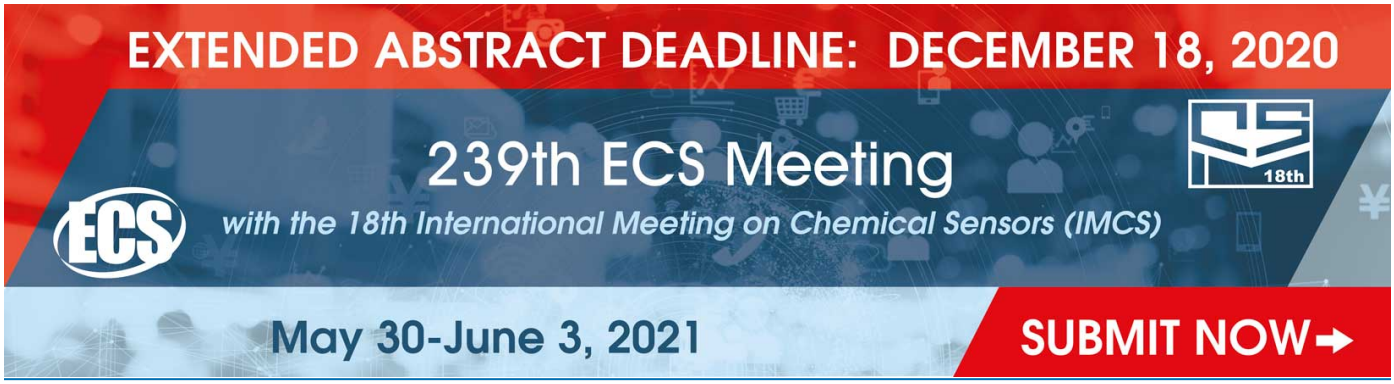
The Electrochemical Society
Advancing solid state & electrochemical science & technology

OPEN ACCESS

CrN/Cr-Coated Steel Plates for High-Temperature Polymer Electrolyte Fuel Cells: Performance and Durability

To cite this article: Ruiyu Li *et al* 2020 *J. Electrochem. Soc.* **167** 144507

View the article online for updates and enhancements.



This content was downloaded from IP address 93.135.145.26 on 07/12/2020 at 19:50

Journal of The Electrochemical Society, 2020 **167** 144507

CrN/Cr-Coated Steel Plates for High-Temperature Polymer Electrolyte Fuel Cells: Performance and Durability

Ruiyu Li,[1,2,=,z] Yun Cai,[1,=] Uwe Reimer,[1] Klaus Wippermann,[1] Zhigang Shao,[2] and Werner Lehnert[1,3]

[1]*Institute of Energy and Climate Research (IEK-14), Forschungszentrum Jülich GmbH, Jülich 52425, Germany*
[2]*Fuel Cell System and Engineering Laboratory, Dalian Institute of Chemical Physics, Chinese Academy of Sciences, Dalian 116023, People's Republic of China*
[3]*Faculty of Mechanical Engineering, RWTH Aachen University, Aachen 52072, Germany*

This paper investigates the general performance and durability performance of a high-temperature polymer electrolyte fuel cell (HT-PEFC) with CrN/Cr-coated SS316L as bipolar plates and compares this with the bare SS316L and graphite bipolar plates. Polarization curves are conducted every 200 h during the 1000 h durability tests for evaluating the overall performances of the HT-PEFCs with different types of bipolar plates. An electrochemical model based on polarization curves, combined with electrochemical impedance spectroscopy (EIS) and scanning electron microscopy (SEM), is used for understanding the degradation mechanisms at play. The CrN/Cr-coated SS316L bipolar plates show excellent corrosion resistance and performance in a real HT-PEFC. Thereby, the degradation rate decrease from ca. 16% of the highest output power with the bare metallic bipolar plates and graphite bipolar plates to almost zero with the CrN/Cr-coated steel bipolar plate.
© 2020 The Author(s). Published on behalf of The Electrochemical Society by IOP Publishing Limited. This is an open access article distributed under the terms of the Creative Commons Attribution 4.0 License (CC BY, http://creativecommons.org/licenses/by/4.0/), which permits unrestricted reuse of the work in any medium, provided the original work is properly cited. [DOI: 10.1149/1945-7111/abc76c]

Manuscript submitted August 25, 2020; revised manuscript received October 13, 2020. Published November 12, 2020. *This paper is part of the JES Focus Issue on Proton Exchange Membrane Fuel Cell and Proton Exchange Membrane Water Electrolyzer Durability.*

Supplementary material for this article is available online

High-temperature polymer electrolyte fuel cells (HT-PEFCs) are promising devices for both mobile and stationary power plant applications and have attracted much attention from researchers around the world.[1–5] The use of metallic bipolar plates instead of graphite bipolar plates is the key to achieving the miniaturization of HT-PEFCs, further reducing their costs and enhancing their mechanical properties, which constitute the main obstacles for the commercialization and practical implementation of HT-PEFC technology.[6,7] The phosphoric acid-doped polybenzimidazole (PBI) membranes as the electrolyte and high operating temperatures (120 °C–180 °C) create a fairly aggressive environment for the components inside HT-PEFCs, especially for metallic bipolar plates. The high corrosion current densities and intense passive layers on the surface of metallic materials caused by the harsh corrosion environment inside of HT-PEFCs make it unfeasible to directly use bare metallic bipolar plates.[7–9]

Applying a conducting and inert coating on the surface of metallic bipolar plates is an effective way of solving the corrosion problem of metallic materials in fuel cells.[10] There is a large amount of work concerning the coatings of metallic bipolar plates in low-temperature polymer electrolyte fuel cells (LT-PEFCs), and coated metallic bipolar plates in LT-PEFC have achieved commercialization.[11–15] The far harsher corrosion environment in an HT-PEFC means that most work concerning metallic bipolar plates in LT-PEFCs could not be directly used for HT-PEFCs. However, there are very few activities that address the coatings of the metallic bipolar plate in HT-PEFCs. Research work concerning the coatings of metallic bipolar plates has mainly focused on three types of coating: doped diamond-like coatings,[16] precious or rare metal coatings[8,17,18] and conductive ceramic coatings.[19,20] Among these coating types, the non-precious ceramic coating, bilayer CrN/Cr, previously reported by our group, has shown the highest potential in the industry application after taking the technical and economic aspects into account.[20]

We investigate the corrosion resistance of the bi-layer CrN/Cr coating in the simulated HT-PEFC environment (85 wt% H_3PO_4 at RT and 130 °C) and conclude that the corrosion current densities of CrN/Cr coated SS316L bipolar plates are circa (ca.) 0.01 and 0.1 $\mu A\ cm^{-2}$, respectively.[20] Moreover, the interfacial contact resistance (ICR) of the bilayer CrN/Cr-coated SS316L bipolar plates is lower than 10 $m\Omega\ cm^{-2}$.[20] The target of the U.S. Department of Energy (DOE) for the corrosion rate and ICR of metallic bipolar plates in PEFC is less than 1.0 $\mu A\ cm^{-2}$ and 10 $m\Omega\ cm^{-2}$, respectively. Therefore, the CrN/Cr-coated SS316L bipolar plates appear promising as low-cost metallic bipolar plates for application in HT-PEFCs. Except for the excellent corrosion resistance and ICR of the bi-layer CrN/Cr coating in the simulated HT-PEFC environment, the CrN/Cr coating also shows self-healing ability in the simulated HT-PEFC environments when defects appeared on the surface of coating, which is vital for the long-term application in the harsh environment of HT-PEFC.[21] For coatings without self-healing ability should be very hard to survive in the harsh environment of HT-PEFC, since the electrolyte will pass through the defects area and contact with the metallic substrate, severe localized corrosion will happen and the whole coating failed finally.[21]

The aim of this work is for the first time to characterize the durability and performance of a non-precious coating modified metallic bipolar plates (CrN/Cr-coated SS316L) in a real HT-PEFC and to compare this with the overall performance of HT-PEFCs constructed with the bare SS316L and graphite bipolar plates. The modeling of polarization curves and electrochemical impedance spectroscopy (EIS) were conducted in situ to investigate the effect of different bipolar plates on the degradation mechanism of HT-PEFCs. Additionally, the surface morphologies of the bare and coated metallic bipolar plates after 1000 h durability tests were measured and compared.

Experimental

A single cell setup from balticFuelCell GmbH (quickCONNECT fixture) was chosen and details about this test cell can be found in the balticFuelCells user manual. Adapted flow field plates with an active area of 25 cm^2 and a serpentine channel structure on both the anode

[=]These authors contributed equally to this work.
[z]E-mail: ruiyu.li@outlook.com

and cathode sides were developed at the IEK-14 (Forschungszentrum Jülich) to fit into the Baltic Module, as shown in Fig. 1. The test rig used in this work is an automated test rig that was also developed at the IEK-14, and Rahim et al. have published the details about it.[22] Three different sets of bipolar plate materials were used, namely: bare SS316L, CrN/Cr-coated SS316L and graphite. The metallic and graphite bipolar plates were fabricated by the machinery method. The CrN/Cr coating was deposited on the surface of bare SS316L bipolar plates by using a magnetron sputtering method at Teer Coating Ltd.[20] In brief, firstly, an adhesion 0.2 μm thick Cr layer was deposited, following by the forming of outside CrN layer by introducing nitrogen into the chamber during sputtering.[23] Finally, the CrN/Cr coating is composed of two layers: an inner Cr layer and an outer CrN layer; the thickness of the CrN/Cr coating is ca. 2 μm,[20] as shown in Fig. 2.

Identical PBI-based Dapozol® 101 membrane-electrode assemblies (MEAs) with an active area of 21 cm^2 from Danish Power Systems (DaPoSy) were employed in this study. The cells were operated at 160 °C under atmospheric pressure with H_2/air and a stoichiometry of $\lambda_{H2/air}$ = 2/2.5. The MEAs were initially run for break-in purposes at constant load (200 mA cm^{-2}) for 70 h. Then, a durability test of 1000 h was carried out under constant load (200 mA cm^{-2}). Furthermore, polarization curves were performed every 200 h. To distinguish and quantify various sources of polarization loss in HT-PEFCs with different types of bipolar plate, EIS measurements were also carried out every 200 h under the current density of 200 mA cm^{-2}, which is the typical current density for the long term operation of an HT-PEFC. The EIS measurements were conducted with an IM 6 unit from Zahner Elektrik in a frequency range of 100 kHz-50 mHz and an amplitude of 10 mV. THALES software was used to fit the impedance data with a simple equivalent circuit (EC), shown in Fig. 7a. R_{ohm} is the ohmic resistance of the system, which is mainly dominated by the resistance of proton transport in the membrane and the interfacial contact resistance (ICR).[24] Meanwhile, R_{ct} represents the charge transfer resistance of the oxygen reduction reaction (ORR).[25,26]

The morphologies and compositions of bare SS316L and CrN/Cr-coated SS316L bipolar plates were investigated under magnification using a Zeiss Gemini Ultra Plus scanning electron microscope (SEM) and energy dispersive X-ray spectroscopy (EDX) before and after 1000 h durability tests. Figure 3 shows the SEM of fresh bipolar plates without durability tests, and the related main compositions measured by EDX are shown in Table I.

Results and Discussion

Cell performance.—Three single cells with graphite bipolar plates, bare and CrN/Cr-coated SS316L bipolar plates were investigated under galvanostatic operation at 0.2 A cm^{-2} for 1000 h. In order to evaluate the overall performance of the single cells before and after the 1000 h durability tests, we recorded polarization curves at different current densities every 200 h (see appendix, Fig. A1 is available online at stacks.iop.org/JES/167/144507/mmedia). The polarization curves at the beginning of life (BOL) and end of life (EOL) are shown in Fig. 4. At BOL, the single cell with graphite bipolar plate showed the best performance amongst the three cells, while the single cell with a bare SS316L bipolar plate showed the worst. This is reasonable, because the ICR values of graphite bipolar plates are the lowest at the initial state amongst all three types of bipolar plates, while the bare SS316L shows highest.[20] After 1000 h durability tests under a constant current of 0.2 A cm^{-2}, the single cell with CrN/Cr-coated SS316L showed the best performance, which almost overlaps with the initial polarization curve at BOL. While, for cases of graphite bipolar plate and bare SS316L bipolar plates, the single cells showed an apparent degradation with a ca. 16% loss of the maximum power output after 1000 h running time. This indicates that the bilayer CrN/Cr coating gives an excellent protective effect on the metallic bipolar plate and superb performance inside a real HT-PEFC.

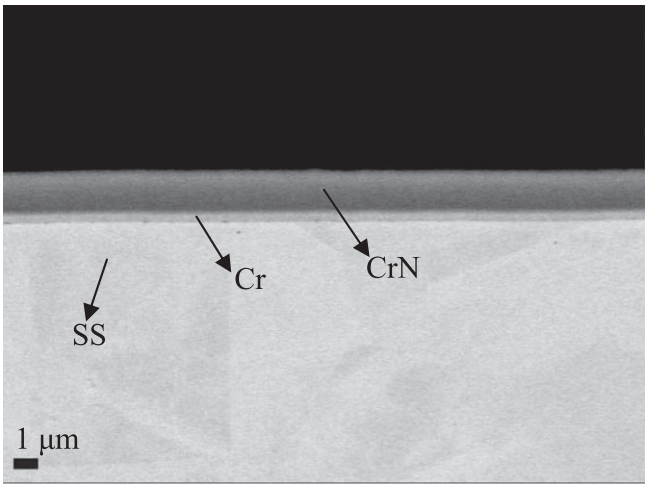


Figure 2. The cross-section image of the Cr/CrN coating.

Modeling analysis of polarization curves—The polarization curves have been analyzed with the basic model shown in Eq. 1 [27,28] in order to inform the identification of the main degradation effect, the cell voltage (E_{cell}) is given by the following equation.

$$E_{cell} = E_{OCV} - R_{ohm} \cdot j - \eta_{act}(j) - \eta_{trans}(j) \quad [1]$$

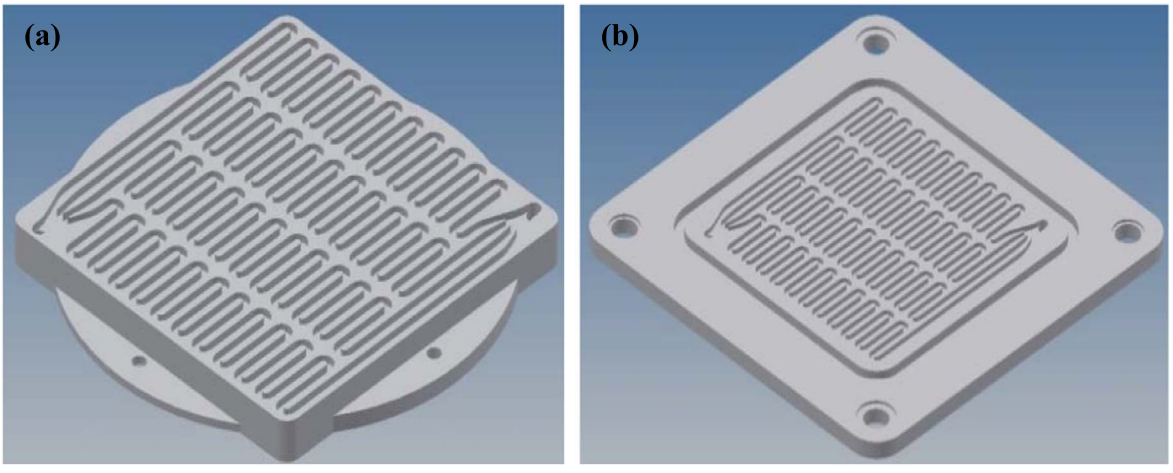


Figure 1. Drawing of bipolar plates: (a) flow field plate for the anode side of an HT-PEFC; (b) flow field plate for the cathode side of an HT-PEFC.

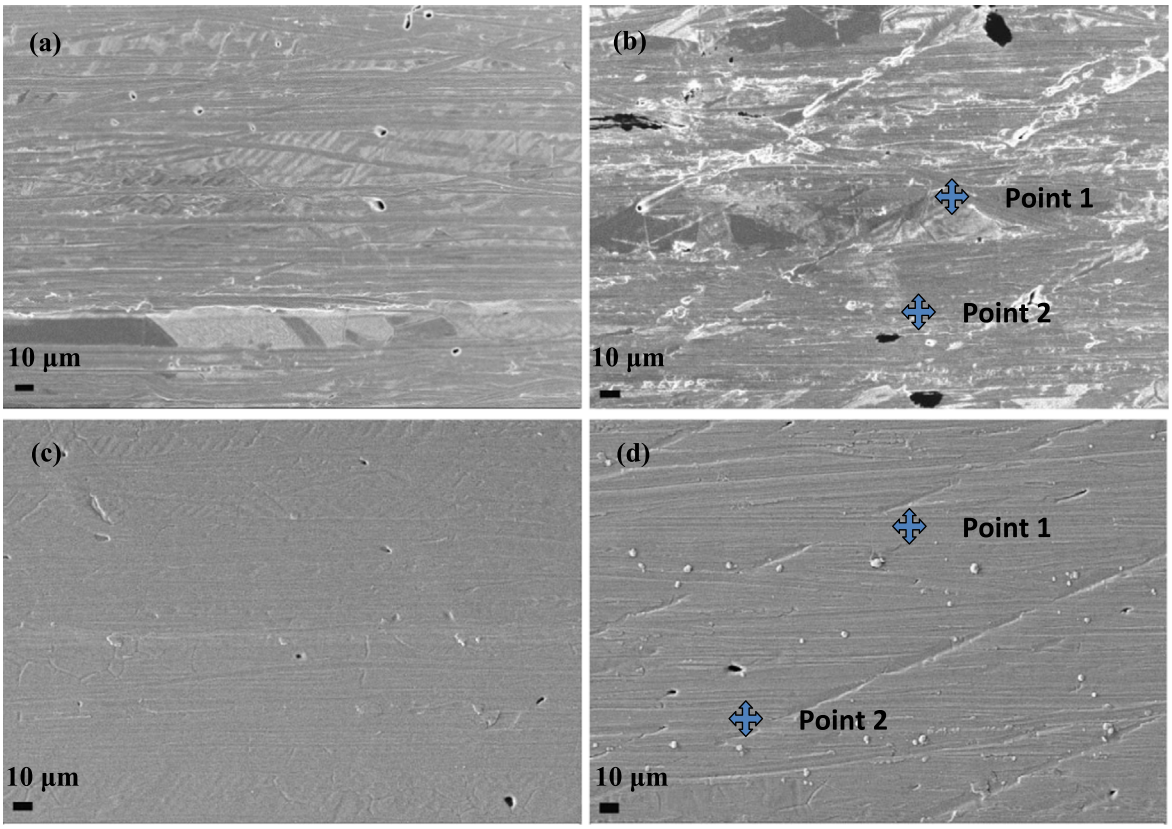


Figure 3. SEM of fresh bipolar plates: (a) channel of bare SS316L bipolar plates; (b) land of bare SS316L bipolar plates; (c) channel of CrN/Cr-coated SS316L bipolar plates; (d) land of CrN/Cr-coated SS316L bipolar plates.

Table I. EDX data (in wt%) of the bare and coated SS316L before and after the 1000 h durability test as shown in Figs. 2 and 7, separately.

Sample	Measure point	O	N	P	Cr	Fe	Ni
SS316L	Cathode land& point 1	\	\	\	17.8	68.7	9.2
SS316L	Cathode land& point 1-after	51.1	\	22.8	3.2	21.1	1.6
SS316L	Cathode land& point 2	\	\	\	18.1	67.4	9.8
SS316L	Cathode land& point 2-after	14.1	\	2.8	15.6	54.8	9.6
Coated SS316L	Cathode land& point 1	\	11.9	\	87.2	0.4	\
Coated SS316L	Cathode land& point 1-after	\	11.7	\	87.8	0.5	\
Coated SS316L	Cathode land& point 2	\	11.3	\	87.8	0.3	\
Coated SS316L	Cathode land& point 2-after	39.5	\	31.2	4.6	3.08	17.4

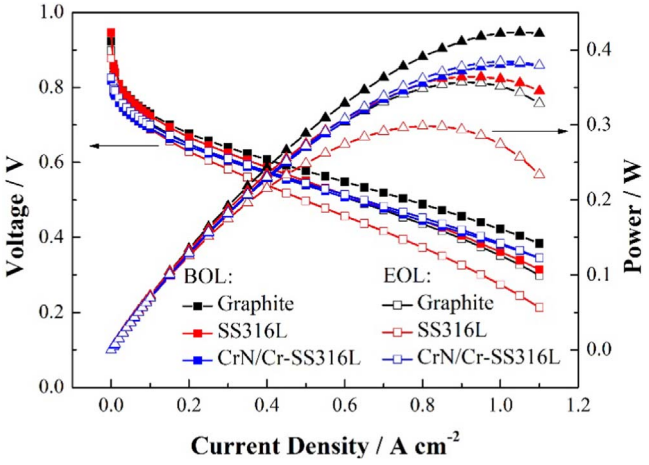


Figure 4. Polarization curves of the single cells at BOL and EOL.

Here, R_{ohm} represents the ohmic resistance, and j gives the current density. The model uses open circuit voltage (E_{ocv}) instead of Nernst voltage. The activation losses (η_{act}) and mass transport losses (η_{trans}) are defined in Eqs. 2 and 3:[27,28]

$$\eta_{act}(j) = \frac{R \cdot T}{\alpha \cdot F} \ln\left(\frac{j}{j_0}\right) \quad [2]$$

$$\eta_{trans}(j) = \frac{R \cdot T}{2 \cdot F} \ln\left(\frac{j_{lim}}{j_{lim} - j}\right) \quad [3]$$

Where, α represents the effective symmetry factor, T represents the operating temperature, j_{lim} is the limiting current density, j_0 is the exchange current density.

The analysis was performed in two steps. In the first, the model was fitted in the low current region of 0.006 A cm^{-2} to 0.135 A cm^{-2}. In this region, the polarization curve is dominated by the activation loss as described by the Tafel equation (Eq. 2). For

such low currents, it can be assumed that $\eta_{trans} = 0$. For the fitting procedure, the value of η_{act} was calculated from Eq. 1 by assuming an average ohmic resistance of $R_{ohm} = 0.2\ \Omega\ cm^2$. This value had very little influence on the fitting results and could be changed by +/−50% without any significant effect. All polarization curves showed an almost perfect linear relationship in this current density region. Figure 5 shows the fit for the graphite plates at the beginning of life. All other fits were of similar quality. The resulting values are displayed in Table II. The data contain some noise, as explained above, but it can be clearly discerned that there is no obvious degradation of the catalyst, as indicated by the virtually constant exchange current densities. It should also be noted that the voltage loss depends on the logarithm of j_0 (see Eq. 2).

In the next step, the parameters R_{ohm} and j_{lim} were fitted. For this purpose, constant values of α and j_0 from the Tafel plots were chosen, as shown in Table II. The resulting curves are presented in Fig. A1 in the Appendix for reference. The overall fit of the polarization curves can be regarded as satisfactory. The relative changes in ohmic resistances are shown in Fig. 6a. For graphite and SS316L, a continuous increase of resistance was observed. Overall, the value of R_{ohm} increased in both cases by 10%. The ohmic resistance of CrN/Cr-SS316L must be considered to remain more or less constant. The parameter j_{lim} also seems to remain constant for CrN/Cr-SS316L in Fig. 6b. Moreover, the limiting current densities for graphite and SS316L decrease by roughly 10%.

An increase in the ohmic resistance indicates a loss of phosphoric acid from the MEA. It has been observed before that phosphoric acid migrates from the MEA and creeps through the GDL towards the flow field plates.[18,29–31] As the acid moves through the GDL, it blocks some of the porous space, which is necessary for gas transport.[31] This leads to a decrease in the limiting current density. It is known that graphite plates take up a considerable amount of acid due to their intrinsic porosity.[18] Stainless steel plates, such as SS316L, react with phosphoric acid, which leads to corrosion products at the surface and, finally, to the disintegration of the structure.[11,12] After corroding, the surface of bare SS316L will also become porous, which will increase the uptake of phosphoric acid. From the results above, it can be concluded that the main degradation phenomenon is the loss of phosphoric acid for graphite and bare SS316L bipolar plates, as these plates have a mechanism for acid uptake. The coated CrN/Cr-SS316L does not show such degradation. This is reasonable, because due to the excellent corrosion resistance of the CrN/Cr coating in the environment of an HT-PEFC,[20] the corrosion phenomenon of the bipolar plates will be dramatically weakened. And, due to the compact of conductive ceramic coating, such as the CrN/Cr coating, the effect of the uptake of phosphoric acid on the membrane's conductivity due to the porosity of bipolar plates should be diminished.

EIS.—After being simulated by using the EC in Fig. 6a, two types of resistance could be extracted from the EIS spectra, as shown in Figs. 7b and 7c. Figure 7b gives the R_{ohm} of all three HT-PEFCs every 200 h during the 1000 h durability tests. The R_{ohm} of the single cells with bare SS316L bipolar plates continuously increased during the 1000 h durability tests, and yields the highest value of R_{ohm}. While, even though the R_{ohm} of the single cells with graphite bipolar plates firstly decreased during the 1000 h durability tests, but finally increased after 1000 h durability tests. In contrast, the R_{ohm} of the single cell with CrN/Cr-coated SS316L bipolar plates exhibited slightly decrease during the 1000 h durability tests. The mechanism of the different behaviors of ohmic resistance of HT-PEFCs constructed with different types of bipolar plates has been explained in above. The slightly difference between the EIS results and the modeling results might come from the redistribution of phosphoric acid during the polarization curves, but the overall trends are similar with each other.

The change of R_{ct} in the three HT-PEFCs with different bipolar plates every 200 h during the 1000 h durability tests is shown in Fig. 7c. The R_{ct} is mainly influenced by the kinetics of the oxygen reduction reaction (ORR) process. By comparison, the R_{ct} of the HT-PEFCs with graphite and bare SS316L bipolar plates increased after 1000 h durability tests. In contrast, the R_{ct} of the HT-PEFC with CrN/Cr-coated SS316L bipolar plates decreased after the 1000 h durability test. In a normal situation, the catalyst powders will agglomerate and grow larger during the running of the fuel cell, which results in a decrease in the electrochemically-active surface area (EASA).[26] The decrease in the EASA will result in a decrease in the exchange current density, which leads to an increase in R_{ct}.[26] This is the case for all three HT-PEFCs. While the EASA is directly determined by the three-phase boundary, which must not only consider the size of the catalyst powders, but also the amount of phosphoric acid in the catalyst layer. As is mentioned above, the porosity of graphite bipolar plates and corroded bare SS316L bipolar plates will absorb the phosphoric acid from the catalyst layer and membrane. The acid loss from the catalyst layer will also reduce the EASA.[18] Therefore, it is reasonable for an increase of R_{ct} and relatively lower exchange current density (as is shown in Table II) of the HT-PEFCs with graphite and bare SS316L bipolar plates. In the case of CrN/Cr-coated SS316L bipolar plates, the uptake of phosphoric acid by bipolar plates is weakened due to the compact surface of the ceramic coating. Therefore, the additional phosphoric acid of the leaching from the membrane during operation will move to the catalyst layer. The increase of phosphoric acid content in the catalyst layer will increase the amount of the three-phase boundary, which increases the EASA. Finally, the interaction of the growth of the catalyst powders and the increase in the phosphoric acid of the catalyst layer might result in a balance of the EASA. Therefore, the R_{ct} of the HT-PEFC with CrN/Cr-coated SS316L bipolar plates remains almost constant, as is shown in Fig. 7c.

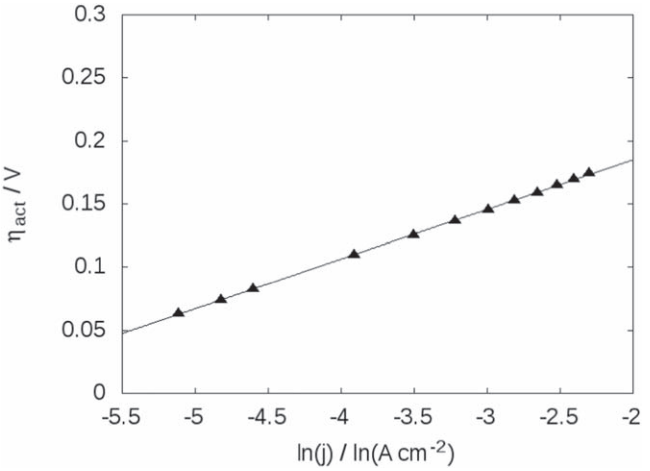


Figure 5. Tafel plot for graphite plate cell at the beginning of life with triangles(experiment) and line(fit).

SEM.—The pictures of the SEM of bare SS316L after the 1000 h durability test are shown in Figs. 8a∼8d. These show that the corrosion products appear on almost all of the surfaces, which indicates a severe corrosion attack on the bare metallic bipolar plates. The corrosion products are mainly metal phosphates, as shown in Table I. Therefore, the direct use of bare metallic bipolar plates will not be possible for HT-PEFCs for long-term application.

Figures 8e ∼ 8h show the surface morphologies of the CrN/Cr-coated SS316L bipolar plate after the 1000 h durability test. It is apparent that the surface is much cleaner compared to the bare one; most of the coated surface is free of corrosion product. On the anode side of the HT-PEFC, the CrN/Cr-coated metallic bipolar plate is free of corrosion products, while there are some slight corrosion products on the surface of the bipolar plate on the cathode side of the HT-PEFC, and they are also mainly metal phosphates (as shown in Table I). This may indicates that the environment on the cathode side

Table II. Selected fitting values and the fitting results for the low current density region (0.006 A cm^{-2} to 0.135 A cm^{-2}).

	Graphite		SS316L		CrN/Cr-SS316L	
time/h	α	j_0/A cm^{-2}	α	j_0/A cm^{-2}	α	j_0/A cm^{-2}
0	0.96	0.0012	0.89	0.00083	1.35	0.0026
200	1.0	0.0016	1.0	0.0011	1.18	0.0036
400	1.0	0.0015	0.89	0.0011	1.22	0.0035
600	0.98	0.0016	0.91	0.0011	1.23	0.0038
800	0.92	0.0017	0.97	0.0017	1.27	0.0037
1000	1.0	0.0016	0.98	0.0019	1.24	0.0037
selected	0.98	0.0015	0.94	0.001	1.23	0.003

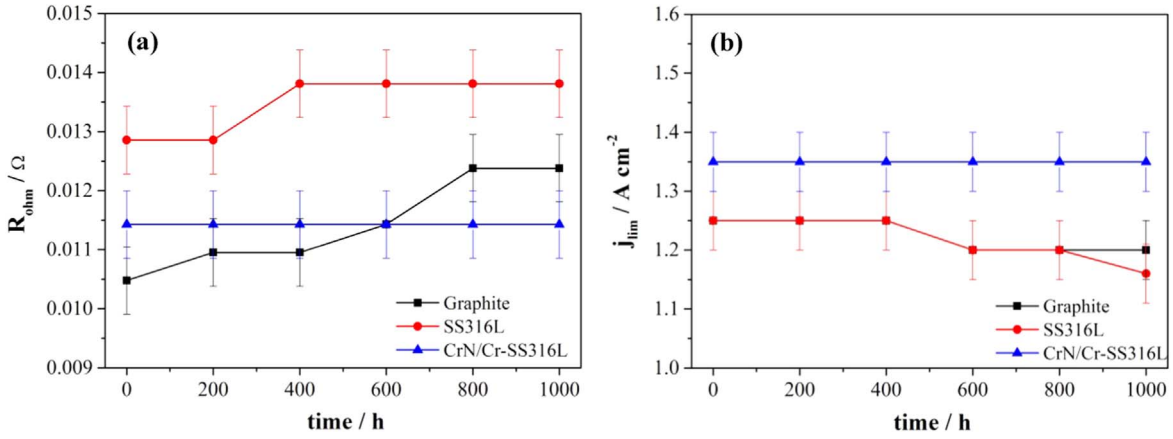


Figure 6. Fitting results of R_{ohm} and j_{lim}: (a) relative change of R_{ohm} over time; (b) relative change of j_{lim} over time.

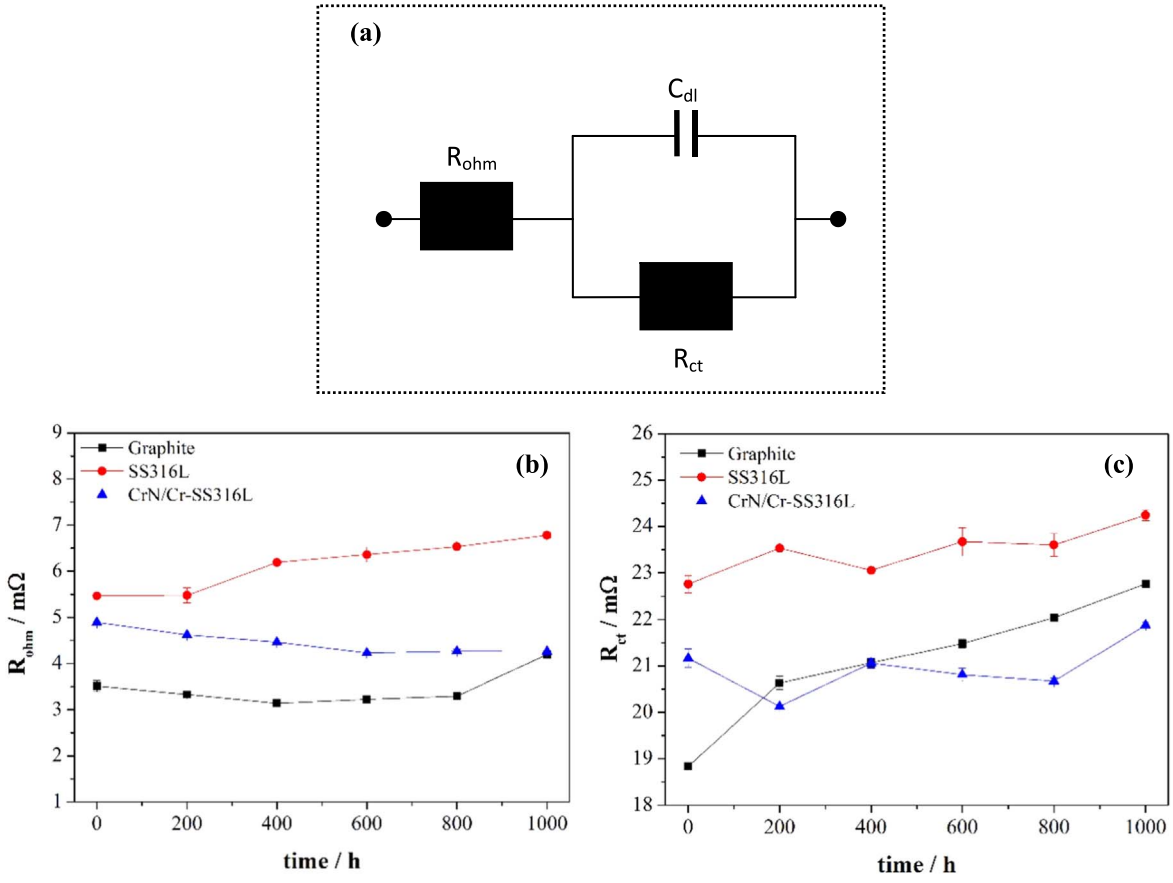


Figure 7. The comparison of resistances (R_{ohm} and R_{ct}) of HT-PEFCs with different bipolar plates: (a) EC for fitting; (b) R_{ohm}; (c) R_{ct}.

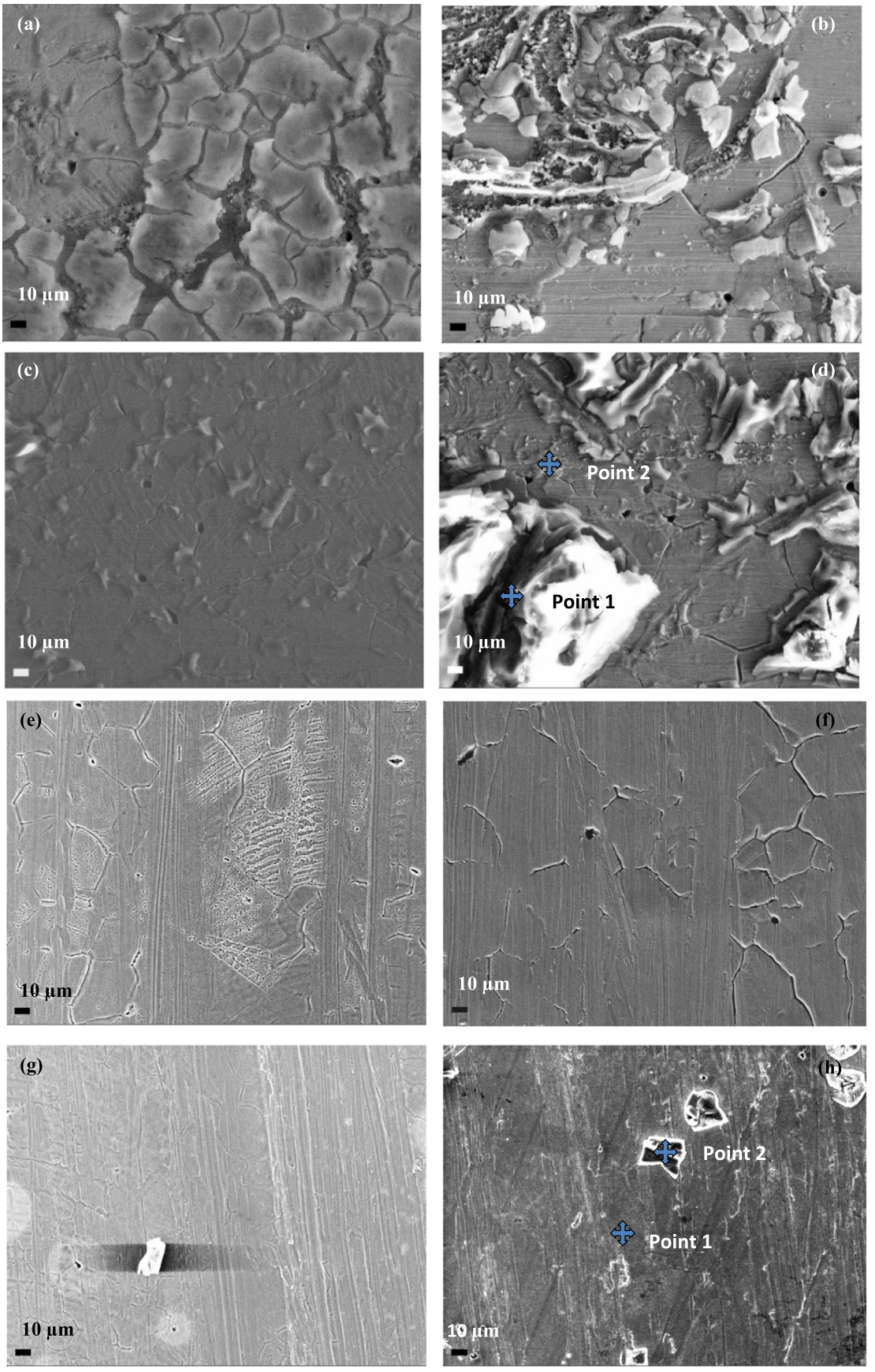


Figure 8. SEM of SS316L bipolar plates and CrN/Cr-coated SS316L bipolar plates after 1000 h durability tests: (a) channel of the anode side (bare SS316L); (b) land of the anode side (bare SS316L); (c) channel of the cathode side (bare SS316L); (d) land of the cathode side (bare SS316L); (e) channel of anode side (CrN/Cr-SS316L); (f) land of the anode side (CrN/Cr-SS316L); (g) channel of the cathode side (CrN/Cr-SS316L); (h) land of the cathode side (CrN/Cr-SS316L).

is more severe than on the anode side, as in the case of a CrN/Cr coating in a real HT-PEFC. There may be three effects: the producing of water on the cathode side could cause more phosphoric acid leaching into the bipolar plate on the cathode side than on the anode side; secondly, the moisture environment will also have a boosting effect on the aggressive environment; also, the potential at the cathode side is easier for producing corrosion products than the anode side of CrN/Cr-coated SS316L. Even though there are some small pieces of corrosion products on the surface of the CrN/Cr coating on the cathode side of an HT-PEFC, this does not influence the ohmic resistance of the single cell. This phenomenon could be explained that the corrosion products formed in the vacancy of a GDL, and the corrosion products in the vacancy of GDLdo not influence the contact area between the bipolar plates and GDL. Therefore, the ohmic resistance of a single cell with CrN/Cr-coated SS316L bipolar plates remains constant during the 1000 h durability test.

Conclusions

This study demonstrated the performance and durability of HT-PEFCs with CrN/Cr-coated SS316L bipolar plates and compared those with bare SS316L and graphite bipolar plates. After receiving the CrN/Cr coating, the performance of an HT-PEFC with metallic bipolar plates enhanced and degradation decreased from ca. 16% with bare SS316L and graphite bipolar plates to almost zero with the coated one. Therefore, the CrN/Cr-coated SS316L bipolar plate is promising for long-term application in HT-PEFCs.

Acknowledgments

We would like to express our thanks to Andreas Everwand for conducting the SEM measurements. We are also obliged to Christopher Wood for proofreading the manuscript. This work was supported by the National Key Research and Development Program of China (2016YFB0101206).

ORCID

Ruiyu Li https://orcid.org/0000-0002-7116-8455
Klaus Wippermann https://orcid.org/0000-0002-5489-9280

References

1. A. Chandan, M. Hattenberger, A. El-Kharouf, S. F. Du, A. Dhir, V. Self, B. G. Pollet, A. Ingram, and W. Bujalski, *J. Power Sources*, **231**, 264 (2013).
2. F. J. Pinar, N. Pilinski, and P. Wagner, *AIChE J.*, **62**, 217 (2016).
3. S. S. Araya, F. Zhou, V. Liso, S. L. Sahlin, J. R. Vang, S. Thomas, X. Gao, C. Jeppesen, and S. K. Kær, *Int J Hydrogen Energ,*, **41**, 21310 (2016).
4. H. Janßen, L. Lüke, W. Lehnert, and D. Stolten, *Int J Hydrogen Energ*, **42**, 11596 (2017).
5. C. Alegre, L. Álvarez-Manuel, R. Mustata, L. Valiño, A. Lozano, and F. Barreras, *Int J Hydrogen Energ*, **44**, 12748 (2018).
6. P. Alnegren, J. G. Grolig, J. Ekberg, G. Goransson, and J. E. Svensson, *Fuel Cells*, **16**, 39 (2016).
7. V. Weissbecker, K. Wippermann, and W. Lehnert, *J. Electrochem. Soc.*, **161**, F1437 (2014).
8. M. Kouril, E. Christensen, S. Eriksen, and B. Gillesberg, *Mater. Corros.*, **63**, 310 (2012).
9. R. Li, Y. Cai, K. Wippermann, and W. Lehnert, *J. Electrochem. Soc.*, **165**, 8 (2018).
10. R. Li, Y. Cai, K. Wippermann, and W. Lehnert, *ECS Trans.*, **85**, 585 (2018).
11. R. A. Antunes, M. C. L. Oliveira, G. Ett, and V. Ett, *Int J Hydrogen Energ*, **35**, 3632 (2010).
12. K. Feng, Z. G. Li, H. L. Sun, L. Yu, X. Cai, Y. X. Wu, and P. K. Chu, *J. Power Sources*, **222**, 351 (2013).
13. H. B. Zhang, G. Q. Lin, M. Hou, L. Hu, Z. Y. Han, Y. Fu, Z. G. Shao, and B. L. Yi, *J. Power Sources*, **198**, 176 (2012).
14. N. D. Nam and J. G. Kim, *Jpn. J. Appl. Phys.*, **47**, 6887 (2008).
15. Y. Mori, M. Ueda, M. Hashimoto, Y. Aoi, S. Tanase, and T. Sakai, *Surf. Coat. Technol.*, **202**, 4094 (2008).
16. A. Vitali Weissbecker, M. Schulze Lohoff, W. Bauer, Lehnert, and D. Stolten, *20th World Hydrogen Energy Conference 2014," Gwangju, Korea* (2014).
17. H. Janßen, A. Edelmann, T. Mildebrath, P. Müller, W. Lehnert, and D. Stolten, *Int J Hydrogen Energ* (2018).
18. C. Hartnig and T. J. Schmidt, *Electrochim. Acta*, **56**, 4237 (2011).
19. L. Wang, L. Li, H. Liu, S. Wang, H. Fang, H. Gao, K. Gao, Y. Zhang, J. Sun, and J. Yan, *J. Power Sources*, **399**, 343 (2018).
20. R. Li, Y. Cai, K. Wippermann, and W. Lehnert, *J. Power Sources*, **434**, 226718 (2019).
21. Y. C. R. Li, K. Wippermann, and W. Lehnert, *J. Electrochem. Soc.*, **166**, C394 (2019).
22. Y. Rahim, H. Janssen, and W. Lehnert, *Int J Hydrogen Energ*, **42**, 1189 (2017).
23. J. Stallard and D. G. Teer, *Surf Coat Tech*, **188**, 525 (2004).
24. J. L. Jespersen, E. Schaltz, and S. K. Kaer, *J. Power Sources*, **191**, 289 (2009).
25. R. Makharia, M. F. Mathias, and D. R. Baker, *J. Electrochem. Soc.*, **152**, A970 (2005).
26. S. Liu, M. Rasinski, Y. Lin, K. Wippermann, A. Everwand, and W. Lehnert, *Electrochim. Acta* (2018).
27. W. L. U. Reimer, Y. Holade, and B. Kokoh, *In Fuel Cells and Hydrogen—From Fundamentals to Applied Research*, ed. V. H. A. S. Mitsushima (Elsevier, Amsterdam) p. 15 (2018).
28. U. Reimer, B. Schumacher, and W. Lehnert, *J. Electrochem. Soc.*, **162**, F153 (2015).
29. H. Becker, U. Reimer, D. Aili, L. N. Cleemann, J. O. Jensen, W. Lehnert, and Q. Li, *J. Electrochem. Soc.*, **165**, F863 (2018).
30. S. Matar, A. Higier, and H. Liu, *J. Power Sources*, **195**, 181 (2010).
31. S. Eberhardt, F. Marone, M. Stampanoni, F. Büchi, and T. Schmidt, *J. Electrochem. Soc.*, **163**, F842 (2016).